

Preparation of Nitrogen-Doped Porous Carbon from Melamine-Formaldehyde Resins Crosslinked by Phytic Acid

Wei Xiong^{1,2}, Ji Hoon Kang¹, and Yongju Jung^{1,*}

¹ Department of Chemical Engineering, Korea University of Technology and Education (KOREATECH), Cheonan 31253, Republic of Korea

² School of Chemistry and Environmental Engineering, Wuhan Institute of Technology, 693 Xiongchu Road, Wuhan 430073, P. R. China

*E-mail: yjung@koreatech.ac.kr

Received: 17 September 2017 / Accepted: 11 November 2017 / Published: 16 December 2017

A new approach for the fabrication of nitrogen-doped hierarchical porous carbon (NHPC) is presented on the basis of the carbonization of melamine-formaldehyde resins crosslinked by phytic acid. The specific surface area and micropore volume of NHPC greatly increased with an increase in carbonization temperature. The NHPC sample (NHPC-850) synthesized at 850 °C showed a high surface area (2732 m²/g) and a large pore volume (1.46 cm³/g) with hierarchical porous structures of macro-, meso- and micropores. It is thought that phytic acid contributed to increasing the space between carbon frameworks during carbonization. This increase allowed KOH to be more uniformly distributed in the carbon framework, leading to a more effective activation process. NHPC-850 exhibited excellent electrochemical performance in an aqueous 6.0 M KOH solution, including a high specific capacitance (271 F/g at 1.0 A/g), an excellent rate property of 70% at 10.0 A/g, and ~100% retention after 500 cycles.

Keywords: Nitrogen-doped hierarchical porous carbon, melamine-formaldehyde resin, supercapacitor, phytic acid, crosslinker

1. INTRODUCTION

Porous carbon structures, which are commonly used as supercapacitor electrode materials, have many advantages such as low cost, a large surface area, good conductivity and a long cycle life[1-4]. In general, carbon-based electrode materials suffer from low capacitance, which limits their wide application in supercapacitors. To improve the capacitance of carbon electrodes, carbon composite materials have been synthesized, including carbon/metal oxides (e.g., NiO, MnO₂) and

carbon/conducting polymers (e.g., polyaniline and polypyrrole)[5-8]. However, these materials often significantly reduce the cycle stability of electrochemical double layer capacitors (EDLC) compared to that of unmodified carbons. Recently, N-doped porous carbon has received widespread attention due to its potential advantage of excellent electrochemical performance[9-11]. Xue's group prepared N-doped mesoporous carbon using melamine/phenol/ formaldehyde resin and Pluronic F127, as a carbon/nitrogen source and a mesopore template, respectively[9]. The N-doped mesoporous carbon electrodes exhibited a high specific capacitance of 289 F/g at a current density of 0.2 A/g.

Another way to improve the capacitance of carbon-based electrodes is to design and synthesize porous carbon with a high specific surface area and a unique porous channel network. The electrode's electrochemical performance is known to depend significantly on surface property, pore structure and electrolyte access[12-14]. Tong et al. have successfully prepared hierarchical porous carbon by a self-template method, which offered a high specific capacitance of 257 F/g at 0.5 A/g in aqueous KOH[15]. It is generally accepted that hierarchical porous structures (e.g., micro-, meso-, and macropore) greatly improve the capacitive performance of carbon electrode materials. In addition, many studies have shown that mesopores are highly beneficial for electrolyte diffusion towards carbon surfaces[16-18].

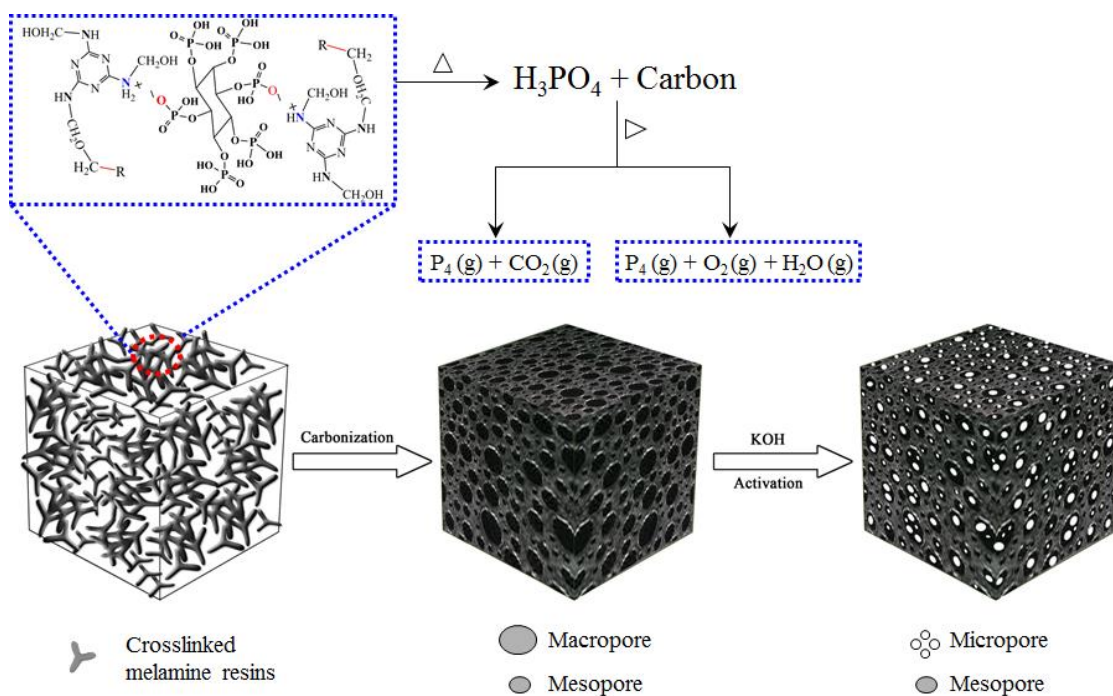


Figure 1. Schematic illustration of the synthesis of NHPC.

Phytic acid has been used as an activating agent to prepare porous carbons[19-21]. Phytic acid is thermally decomposed into inositol and H_3PO_4 during the initial stages of carbonization, and these by-products subsequently generate polyphosphoric acid and P_2O_5 at high temperatures ($> 450\text{ }^\circ\text{C}$). The formation of phosphate linkages serves as a crosslinker between the carbon frameworks, preventing the collapse of pores during carbonization. Moreover, phytic acid has been applied as a protonic acid

dopant to synthesize porous carbon nanofiber networks[22]. Phytic acid is known to expand the spaces between the carbon frameworks during the carbonization process.

In this work, phytic acid is used as a cross-linking agent of a melamine-formaldehyde resin for the synthesis of N-doped hierarchical porous carbon (NHPC) with a large specific surface area, as illustrated in Figure 1. Three different NHPC samples were prepared by varying the carbonization temperature of the cross-linked carbon precursors, followed by an activation process with KOH. The physicochemical properties of the prepared NHPC were analyzed by scanning electron microscopy (SEM), X-ray photoelectron spectroscopy (XPS), and nitrogen adsorption tests. In addition, their electrochemical performance was evaluated in a 6.0 M KOH solution.

2. EXPERIMENTAL SECTION

Melamine, formaldehyde and phytic acid were dissolved in distilled water with a molar ratio of 2:6:1 at 60 °C, followed by vigorous stirring for 30 min. Typically, the mixed solution containing 1.0 M melamine was transferred to an ice bath and stirred for 2 h. The resulting white precipitates were dried under vacuum at -50 °C for 24 h and carbonized in a N₂ environment for 2 h at three different temperatures of 450 °C, 650 °C and 850 °C with a heating rate of 2 °C/min. The carbon samples and KOH were homogeneously mixed with a 1:3 mass ratio, dried and heated in a N₂ environment at 800 °C for 1 h. The final products, denoted as NHPC-450, NHPC-650, and NHPC-850, were obtained after washing activated carbon samples several times to obtain a pH near 7.

FE-SEM images and nitrogen sorption isotherms for the prepared NHPC samples were taken using a JSM-5510LV scanning electron microscopy and a Micromeritics Tristar 3000 analyzer, respectively. The surface area and pore size distribution of the carbon samples were estimated by the Brunauer–Emmett–Teller (BET) and Barrett–Joyner–Halenda (BJH) methods, respectively. The surface analyses of the carbon materials were performed using an X-ray photoelectron spectrometer (XPS, MULTILAB2000, VG). All electrochemical behaviors were tested in 6.0 M KOH with a PGSTAT 302N electrochemical workstation (Eco Chemie B.V., Netherlands) in a three-electrode system. The working electrode was fabricated by pressing a mixture of NHPC (80 wt.%), acetylene black (10 wt.%) and polytetrafluoroethylene (PTFE, 10 wt.%) onto a nickel foam (1 cm x 1 cm) at 20 MPa, dried in an oven at 100 °C and soaked in a 6.0 M KOH solution. Cyclic voltammetry (CV) and galvanostatic charge-discharge tests were carried out in a voltage range of -1.0 V ~ 0 V with an Hg/HgO electrode and the nickel-foam as the reference and counter electrodes, respectively. The specific capacitances of the electrodes at different current densities were measured using discharge curves[23].

3. RESULTS AND DISCUSSION

Figure 2 shows the SEM images of the NHPC samples prepared at different carbonization temperatures. All of the samples possessed big macropores (5 ~ 30 μm), suggesting that the phytic acid

effectively prevented pore collapse[24]. Particularly, NHPC-850 showed more abundant macropores than NHPC-450 and NHPC-650.

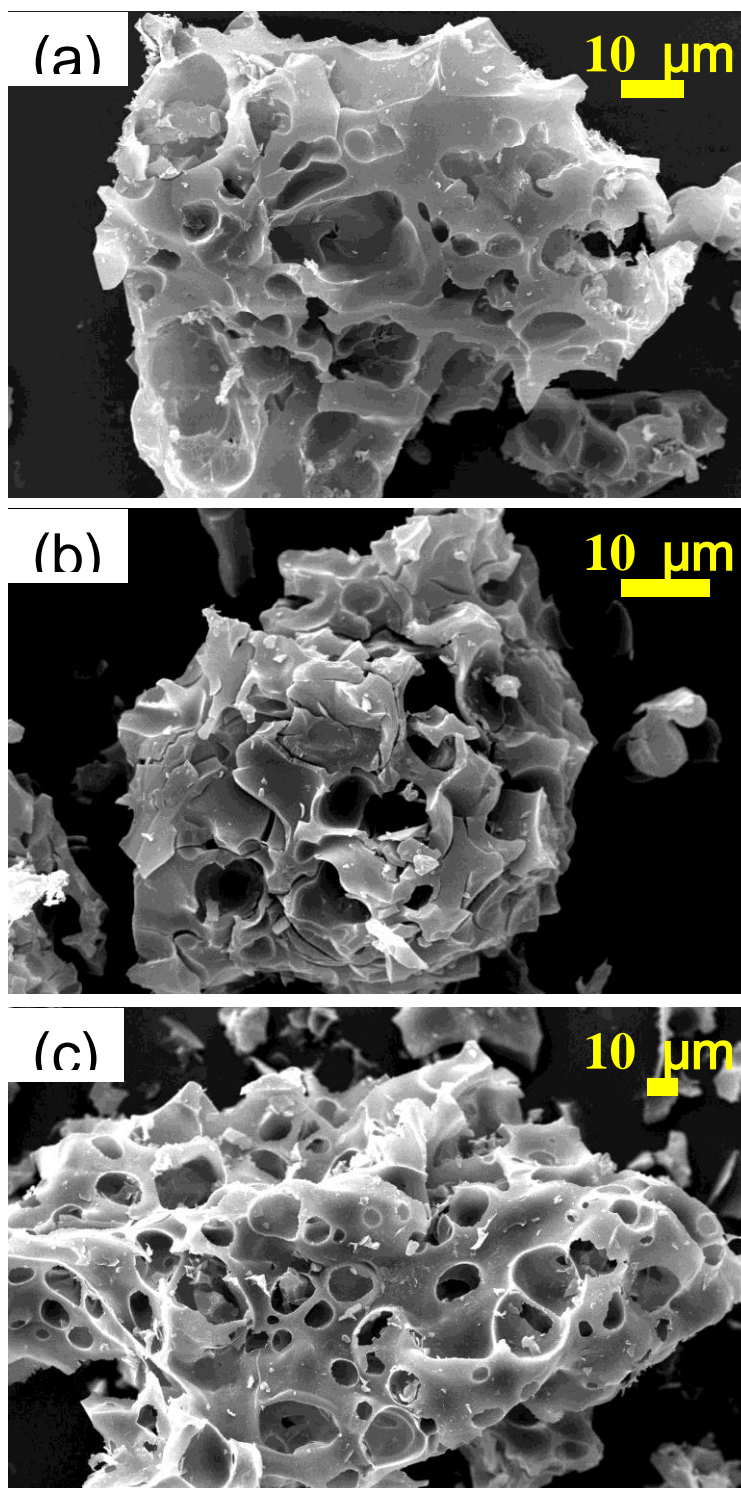


Figure 2. SEM images of NHPC-450 (a), NHPC-650 (b) and NHPC-850 (c).

The microstructural properties of the prepared NHPC samples were further investigated by measuring N₂ adsorption-desorption isotherms at 77 K.

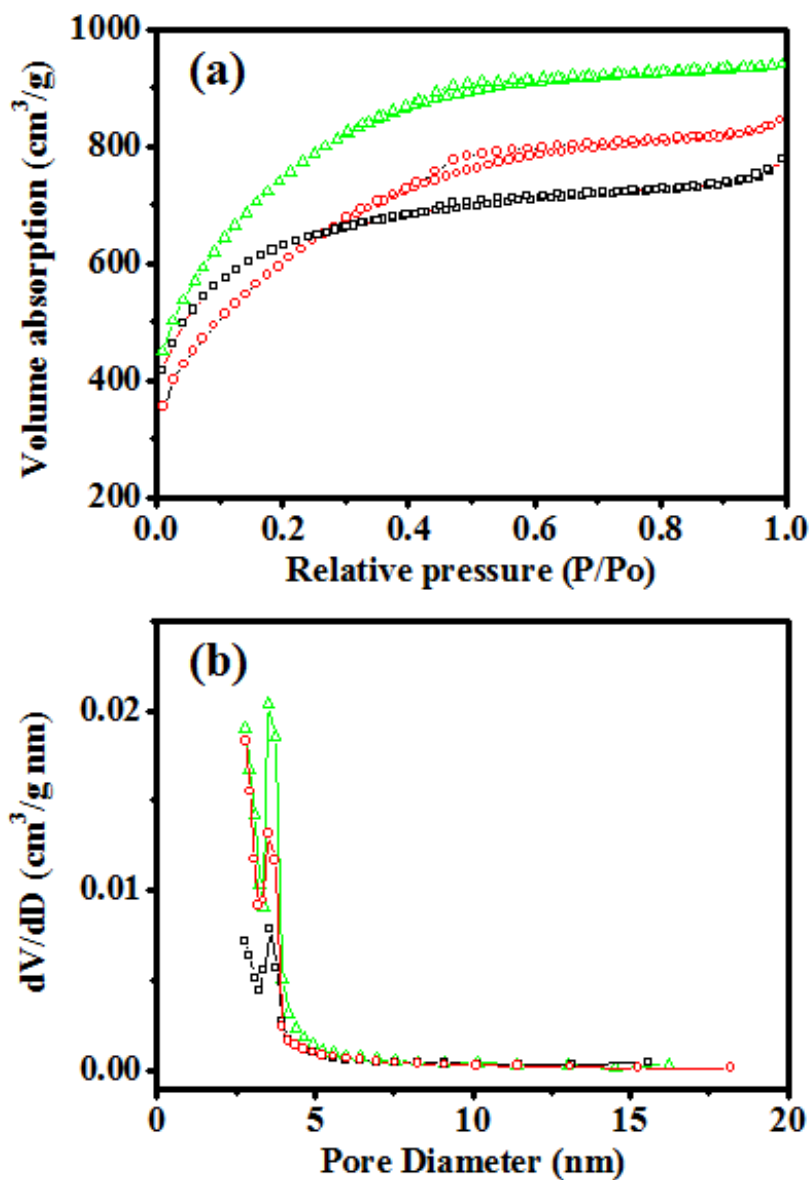


Figure 3. Nitrogen adsorption isotherms (a) and pore size distribution curves (b) of the NHPC samples.

Table 1. Structural properties of nitrogen-doped hierarchical porous carbon.

Sample	S_{BET} (m ² /g)	S_{mic} (m ² /g)	P (nm)	V_{mic} (cm ³ /g)	V_t (cm ³ /g)
NHPC-450	2186	1502	3.5	0.73	1.31
NHPC-650	2307	1996	3.8	0.88	1.20
NHPC-850	2732	2217	3.5	1.05	1.46

S_{BET} , BET surface area; S_{mic} , micropore surface area; P , the most probable pore diameter; V_{mic} , micropore volume; and V_t , total pore volume.

Figure 3a and 3b show nitrogen adsorption isotherms and the corresponding pore size distribution curves, respectively, of the carbon samples as calculated from the desorption branch. Note that all of the samples displayed abundant mesopores (< 20 nm), which may be mainly caused by the decomposition of phytic acid. During carbonization, phytic acid is decomposed into H_3PO_4 and eventually into polyphosphates below 450 °C[20,25]. At higher carbonization temperatures (> 500 °C), the polyphosphates and P_2O_5 react with carbon to generate gaseous products (e.g., P_4 , O_2 , CO_2 , H_2O), which may contribute to the formation of mesopores. As carbonization temperature is increased from 450 to 850 °C, the surface area of the NHPC samples increased from 2186 to 2732 m^2/g (Table 1). NHPC-850 showed a higher surface area and pore volume compared with those of NHPC-450 and NHPC-650 (Table 1). It is thought that the decomposition of phytic acid promoted the formation of porous carbon with a channel structure, which allowed more effective activation with KOH.

Figure 4a shows XPS spectra of the prepared NHPC samples. The peaks for C1s, N1s and O1s were observed at 284.7 , 400.0 and 532.5 eV, respectively[10,26]. The estimated C, O and N contents of the NHPC samples are listed in Table 2. The O and N contents decreased with increasing carbonization temperature, as expected[27]. The chemical states of N in the NHPC were further investigated by fitting the N1s spectra, as shown in Figure 4b-4d. Four peaks with binding energies of nearly 398.0 eV, 400.0 eV, 401.0 eV, and 402.0 eV were assigned as pyridinic-N (N-6), pyrrolic-N (N-5), quaternary nitrogen (N-Q), and pyridine-N-oxide (N-O) functional groups, respectively.

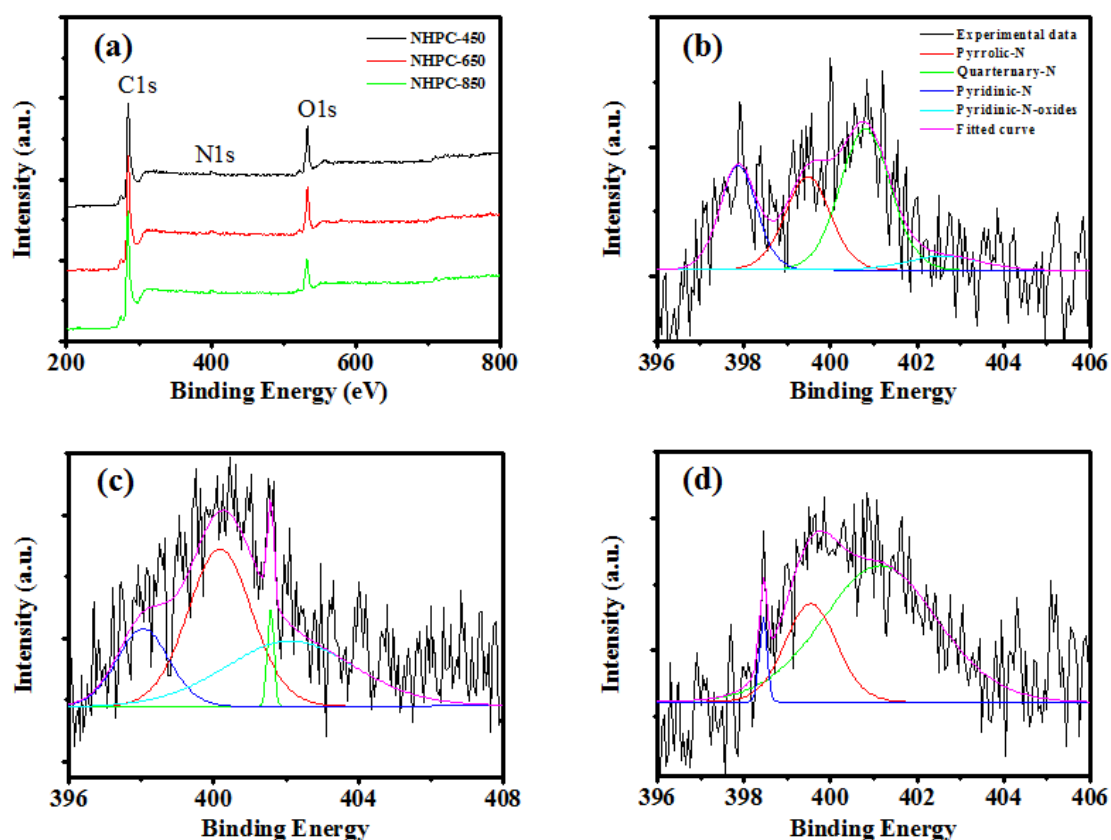


Figure 4. XPS survey spectra of NHPCs (a) and deconvolution results of N1s peaks for NHPC-450 (b), NHPC-650 (c) and NHPC-850 (d).

As the carbonization temperature increased from 450 to 650 °C, the N-Q and N-6 peak intensities became weaker, while the N-5 and N-O peak intensities were greatly increased (Table 2). This feature may be associated with the lower stability of the N-Q and N-6 groups at relatively higher temperatures, whereas some N-Q and N-6 groups can be converted to other nitrogen moieties (e.g., N-5 and N-O). NHPC-850 exhibited a higher N-Q content (73.5%) than the other two samples, which would be beneficial for fast charge transport in carbon electrodes[27,28].

Table 2. Weight percent of surface C, O and N elements, and nitrogen speciation of the nitrogen-doped hierarchical porous carbon, as determined by XPS.

Sample	Weight percentage (%)			Nitrogen moiety (%)			
	C	O	N	N-5	N-6	N-Q	N-O
NHPC-450	75.1	21.8	3.1	26.1	23.8	43.7	6.4
NHPC-650	79.3	18.0	2.7	43.4	17.6	2.7	36.3
NHPC-850	84.7	13.1	2.2	23.6	2.9	73.5	-

N-5, Pyrrolic-N; N-6, Pyridinic-N; N-Q, Quaternary-N; and N-O, Pyridonic-N.

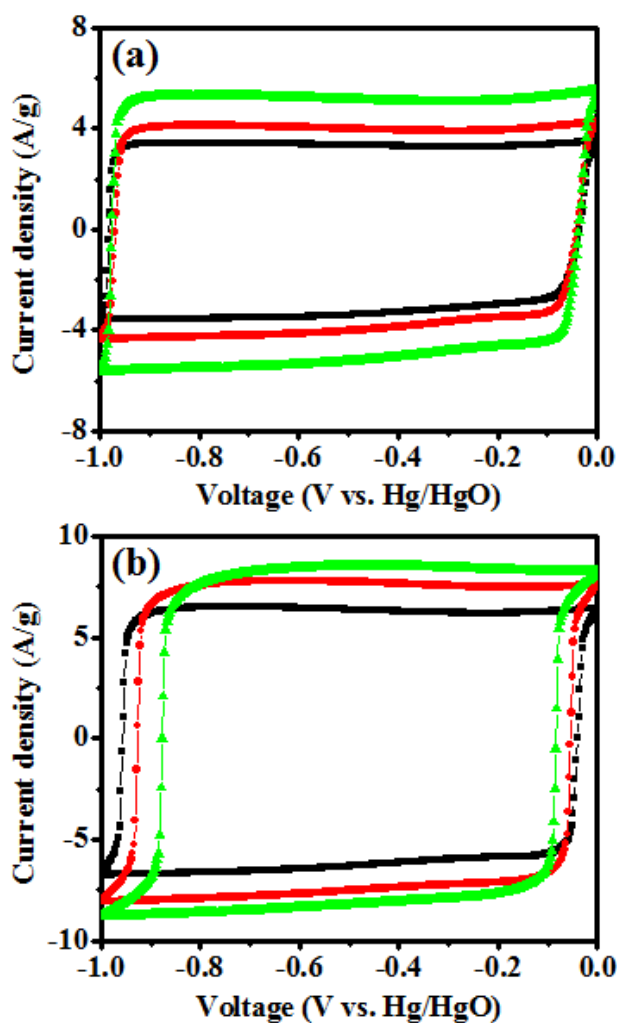


Figure 5. CV curves (a) of NHPC-450 (—), NHPC-650 (—) and NHPC-850 (—) electrodes at 20 mV/s; CV curves (b) of NHPC-850 electrode at 50 (—), 100 (—) and 200 (—) mV/s.

Figure 5a shows CV curves of the NHPC-450, NHPC-650 and NHPC-850 electrodes taken at a scan rate of 20 mV/s. All electrodes showed typical CV curves that are commonly observed in electric double layer capacitors[29]. The NHPC-850 electrode exhibited the largest specific capacitance under the same conditions and maintained the characteristic rectangular CV curve even at a high scan rate of 200 mV/s (Figure 5b), suggesting that the mass transport of the electrolyte occurs rapidly. This feature may be partly due to a large portion of quaternary nitrogen (73.5%) in NHPC-850 (Table 2), which is known to efficiently improve the conductivity of N-doped porous carbon[27].

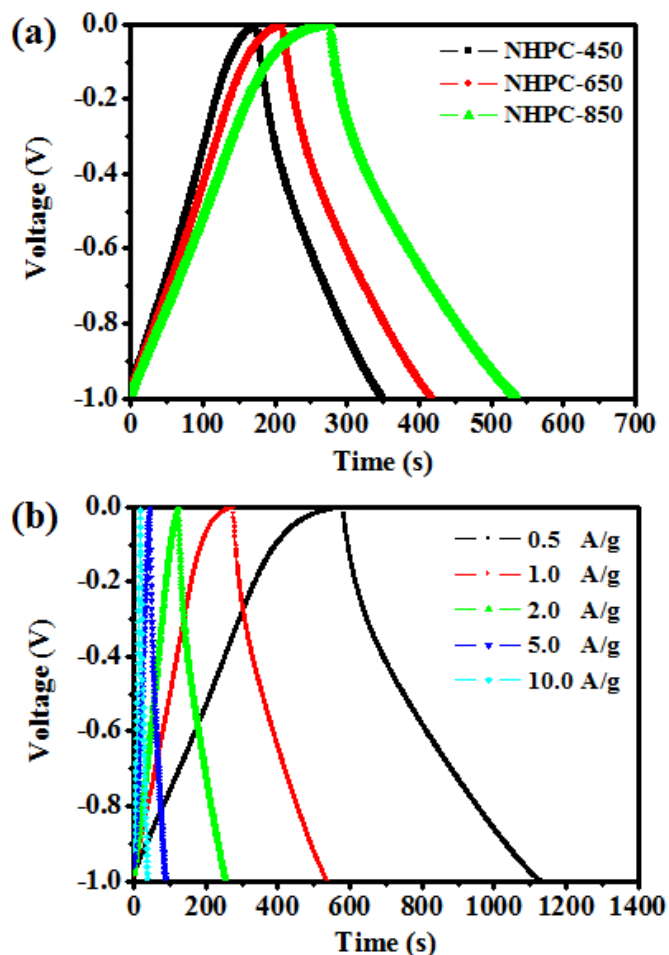


Figure 6. Charge and discharge curves of NHPC-450, NHPC-650 and NHPC-850 electrodes (a); Rate properties of NHPC-850 (b).

Figure 6a shows the charge and discharge curves of the NHPC electrodes at a current density of 1.0 A/g. All charge and discharge curves exhibited isosceles triangular shapes with a slight distortion associated with the pseudocapacitance, which is typically observed in nitrogen-doped porous carbons. NHPC-850 exhibited a much higher specific capacitance of 271 F/g than those of NHPC-450 (175 F/g) and NHPC-650 (208 F/g). Figure 6b shows the charge and discharge curves of the NHPC-850 electrode at different current densities. NHPC-850 exhibited an excellent capacitance of 190 F/g at a significantly high current density of 10 A/g. When compared with previous N-doped carbons, NHPC-

850 exhibited a superior energy storage property and an excellent rate capability (Table 3). These capabilities may be mainly attributed to the hierarchical porous structure with large surface area that allows easy electrolyte access.

Table 3. The electrochemical capacitance values of the prepared nitrogen-doped hierarchical porous carbon and various porous carbon samples.

Samples	C (F/g)					Reference
	0.5 A/g	1.0 A/g	2.0 A/g	5.0 A/g	10.0 A/g	
NHPC-450	206	175	-	-	-	This work
NHPC-650	239	208	-	-	-	This work
NHPC-850	283	271	257	223	190	This work
N-MMCFs	-	198	-	175	168	[30]
NMCs	203 F/g (at 0.1 A/g)					[31]
Carbon-N-1:20	-	219	-	-	-	[32]
N,P-CNWs	-	258	-	-	208	[33]
N-carbons	-	242	-	-	-	[34]

N-MMCFs, Nitrogen-doped carbon foams; NMCs, Nitrogen-doped mesoporous carbons; and N,P-CNWs, N,P-co-doped carbon nanowires.

Cycling stability is also one of the important characteristics for high performance supercapacitor electrodes. The NHPC-850 electrode showed nearly 100% capacitance retention (270 F/g) after 500 cycles (Figure 7).

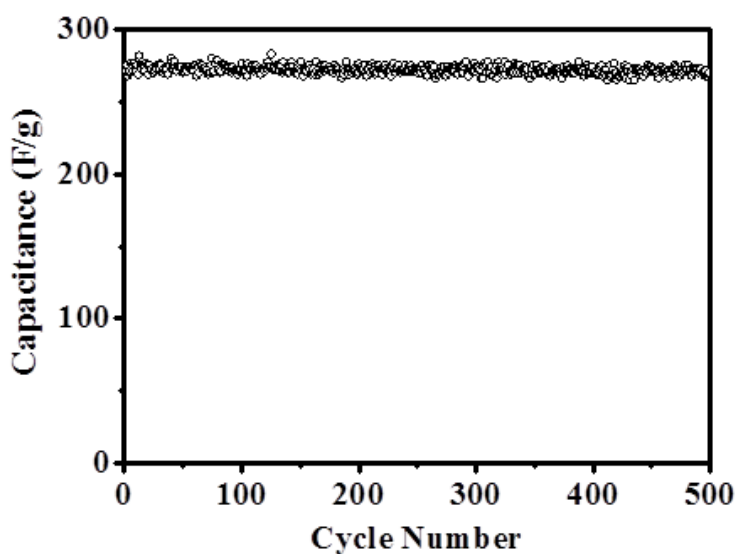


Figure 7. Cycle performance of the NHPC-850 electrode.

4. CONCLUSION

Nitrogen-doped hierarchical porous carbon (NHPC) was successfully prepared through the carbonization of melamine-formaldehyde resins using phytic acid as a crosslinker, followed by subsequent KOH activation to construct a well-developed microstructure. The microstructural property of NHPC was highly sensitive to the carbonization temperature. NHPC-850 showed a significantly high surface area (2732 m²/g) and pore volume (1.46 cm³/g). Additionally, phytic acid may have contributed to the expansion of the space between carbon frameworks, resulting in more effective KOH activation. All NHPC electrodes exhibited charge and discharge curves with slightly distorted isosceles triangular shapes that are caused by the pseudocapacitance originating from the doped nitrogen. NHPC-850 exhibited an outstanding capacitive performance with a high capacitance (271 F/g) and an excellent rate performance (190 F/g at 10 A/g). It is thought that this feature arose from its well-developed hierarchical porous structure and doped nitrogen functional groups.

ACKNOWLEDGEMENTS

This work was supported by the Financial Assistance Programs for Postdoctoral Researchers of KOREATECH.

References

1. Q. Wang, J. Yan and Z.J. Fan, *Energy Environ. Sci.*, 9 (2016) 729.
2. B. Dyatkin, Y. Zhang, E. Mamontov, A.I. Kolesnikov, Y.Q. Cheng, H.M. Meyer, P.T. Cummings and Y. Gogotsi, *J. Phys. Chem. C*, 120 (2016) 8730.
3. M.X. Liu, L.Y. Chen, D.Z. Zhu, H. Duan, W. Xiong, Z.J. Xu, L.H. Gan and L.W. Chen, *Chinese Chem. Lett.*, 27 (2016) 399.
4. W. Xiong, L. Zhou and S.T. Liu, *Chem. Eng. J.*, 284 (2016) 650.
5. M.J. Zhi, C.C. Xiang, J.T. Li, M. Li and N.Q. Wu, *Nanoscale*, 5 (2013) 72.
6. J.S. Qian, H.Y. Jin, B.L. Chen, M. Lin, W. Lu, W.M. Tang, W. Xiong, L.W.H. Chan, S.P. Lau and J.K. Yuan, *Angew. Chem. Int. Ed.*, 54 (2015) 6800.
7. Y.C. Wang, S.Y. Tao, Y.L. An, S. Wu and C.J. Meng, *J. Mater. Chem. A*, 1 (2013) 8876.
8. J.T. Zhang and X.S. Zhao, *J. Phys. Chem. C*, 116 (2012) 5420.
9. M. Li and J.M. Xue, *J. Phys. Chem. C*, 118 (2014) 2507.
10. W.J. Lu, M.X. Liu, J. Miao, D.Z. Zhu, X. Wang, H. Duan, Z.W. Wang, L.C. Li, Z.J. Xu, L.H. Gan and L.W. Chen, *Electrochim. Acta*, 205 (2016) 132.
11. K.N. Wood, R. O'Hayre and S. Pylypenko, *Energy Environ. Sci.*, 7 (2014) 1212.
12. I.S. Ike, I. Sigalas and S. Iyuke, *Phys. Chem. Chem. Phys.*, 18 (2016) 661.
13. E. Redondo, E. Goikolea and R. Mysyk, *Electrochim. Acta*, 221 (2016) 177.
14. Y. Wang, Y. Song and Y. Xia, *Chem. Soc. Rev.*, 45 (2016) 5925.
15. Y.X. Tong, X.M. Li, L.J. Xie, F.Y. Su, J.P. Li, G.H. Sun, Y.D. Gao, N. Zhang, Q. Wei and C.M. Chen, *Energy Storage Mater.*, 3 (2016) 140.
16. J. Zhang, X.B. Yi, W. Ju, H.L. Fan, Q.C. Wang, B.X. Liu and S. Liu, *Electrochem. Commun.*, 74 (2017) 19.
17. D. Feng, Y.Y. Lv, Z.X. Wu, Y.Q. Dou, L. Han, Z.K. Sun, Y.Y. Xia, G.F. Zheng and D.Y. Zhao, *J. Am. Chem. Soc.*, 133 (2011) 15148.

18. J. Cherusseri and K.K. Kar, *J. Mater. Chem. A*, 3 (2015) 21586.
19. Y.Y. Yin, R.Y. Li, Z.J. Li, J.K. Liu, Z.J. Gu and G.L. Wang, *Electrochim. Acta*, 125 (2014) 330.
20. C. Cheng, J. Zhang, Y. Mu, J.H. Gao, Y.L. Feng, H. Liu, Z.Z. Guo and C.L. Zhang, *J. Anal. Appl. Pyrolysis*, 108 (2014) 41.
21. C. Cheng, H. Liu, P. Dai, X. Shen, J. Zhang, T. Zhao and Z. Zhu, *J. Taiwan Inst. Chem. Eng.*, 67 (2016) 532.
22. G. Xu, B. Ding, J. Pan, J. Han, P. Nie, Y. Zhu, Q. Sheng and H. Dou, *J. Mater. Chem. A*, 3 (2015) 23268.
23. P. Yang and W. Mai, *Nano Energy*, 8 (2014) 274.
24. M. Jagtoyen and F. Drbyshire, *Carbon*, 36 (1998) 1085.
25. M. Olivares-Marín, C. Fernández-González, A. Macías-García and V. Gómez-Serrano, *Carbon*, 44 (2006) 2330.
26. M.X. Liu, X.X. Deng, D.Z. Zhu, H. Duan, W. Xiong, Z.J. Xu and L.H. Gan, *Chinese Chem. Lett.*, 27 (2016) 795.
27. Y. Deng, Y. Xie, K. Zou and X. Ji, *J. Mater. Chem. A*, 4 (2016) 1144.
28. T. Lin, I.W. Chen, F. Liu, C. Yang, H. Bi, F. Xu and F. Huang, *Science*, 350 (2015) 1508.
29. F. Bonaccorso, L. Colombo, G. Yu, M. Stoller, V. Tozzini, A.C. Ferrari, R.S. Ruoff and V. Pellegrini, *Science*, 347 (2015).1246501.
30. W. Xiong, M. Liu, L. Gan, Y. Lv, Z. Xu, Z. Hao and L. Chen, *Colloids Surf. A Physicochem. Eng. Asp.*, 411 (2012) 34.
31. H. Chen, F. Sun, J. Wang, W. Li, W. Qiao, L. Ling and D. Long, *J. Phys. Chem. C*, 117 (2013) 8318.
32. X.Y. Chen, D.H. Xie, C. Chen and J.W. Liu, *J. Colloid Interface Sci.*, 393 (2013) 241.
33. Z. Hu, S. Li, P. Cheng, W. Yu, R. Li, X. Shao, W. Lin and D. Yuan, *J. Mater. Sci.*, 51 (2016) 2627.
34. J. Zhu, D. Xu, C. Wang, W. Qian, J. Guo and F. Yan, *Carbon*, 115 (2017) 1.